RoboSub 2026 Technical Design Report

Koło Naukowe SPA i BLSPS — University of Warsaw

J. Balenkowski, M. Bernacki, M. Borowiecki, J. Ciecierski, S. Jezierski, M. Kolecki, A. Lipinska, J. Maleta, M. Malewicz, J. Mikołajczyk, B. Ogórkiewicz

Abstract—For RoboSub 2026, KN SPA i BLSPS presents its first-generation autonomous underwater vehicle (AUV), designed and built from the ground up at the University of Warsaw. The vehicle targets Gate, Avoid Debris (Slalom), and Recon (Bins) as primary tasks, with Torpedo Deployment and Octagon surfacing as secondary goals—selected to maximise reliability under the constraints of a first competition entry. The design philosophy prioritises hardware simplicity and mission robustness: a centralised Jetson Orin compute stack, dedicated RPi + Hailo-8 vision nodes per camera, a spring-loaded dual torpedo launcher, a gravity-release dual marker dropper, and a three-element hydrophone array for acoustic pinger localisation. A key contribution is a Gaussian Splatting synthetic data pipeline that generates annotated underwater training images from pool footage, extending effective YOLO detection range in turbid conditions without additional real-world data collection.

1. Competition & Design Strategy

1.1 Core Strategy

KN SPA i BLSPS enters RoboSub 2026 as a first-time participant. Our core strategic objective is to maximise scoring *reliability* over scoring *potential*. Rather than attempting all five tasks at low success rates, we defined a focused task set where hardware and software capabilities could be validated to high confidence before competition. This sequenced approach is our most critical design trade-off: by constraining scope, we accept a lower theoretical maximum score in exchange for a significantly higher probability of executing attempted tasks correctly within the 15-minute competition window.

Primary targets—Gate, Avoid Debris (Slalom), and Recon (Bins)—rely exclusively on vision-based perception and depth control, the most mature capabilities in our stack. Secondary targets—Torpedo Deployment and Octagon surfacing—extend this foundation with purpose-built actuator systems and acoustic localisation, added in priority order as development time permitted.

1.2 Task–Capability Alignment

Table 1 maps each competition task to the vehicle subsystems required for execution and states our priority level. Subsystems with undetectable or unrecoverable failure modes were excluded from scope. Simpler systems with passive fail-safe behaviour were consistently preferred over more capable but complex alternatives.

Table 1: Task–Capability Matrix

Task	Vis.	Aco.	Drop.	Torp.	Pri.
Gate (I)	✓				1st
Avoid Debris (II)	✓				1st
Recon/Bins (III)	✓		✓		1st
Torpedoes (IV)	✓			✓	2nd
Octagon (V)	✓	✓			2nd

1.3 Role Selection

The vehicle operates in the **Search & Rescue** role throughout the entire competition run. This role is pre-selected before mission start and hard-coded into the mission planner; the vehicle consistently targets the Search & Rescue half of the Gate, the corresponding bins in Task III, the Search & Rescue torpedo board in Task IV, and the correct octagon heading in Task V. Dynamic role classification at runtime was considered but rejected: misclassifying Gate imagery under adverse pool lighting or turbidity would propagate errors to all subsequent tasks. A fixed preselected role eliminates this failure mode entirely, at the cost of forfeiting the theoretical benefit of adaptive role selection.

2. Mechanical Design

2.1 Design Objectives and Frame Architecture

The mechanical frame was designed under strong constraints of development time and budget, prioritising low cost, manufacturability, ease of assembly, and fast iteration. The vehicle is an eight-thruster AUV with full 6-DOF control. The structure is an open-frame rectangular layout (Fig. 1) with four main printed plates: two side plates, a top plate, and a bottom plate. Perforated through-holes reduce mass and allow water to pass freely. Plates connect via rectangular tabs in matching slots, reinforced with galvanised steel angle brackets and M5 screws.

The electronics pressure hull (acrylic tube, ≈500 mm long, 180 mm diameter) is mounted centrally on dedicated supports. Four vertical thrusters pass through the top plate with matching clearance holes in the bottom plate; four horizontal thrusters are mounted on 45° arms attached to the bottom plate, following the ArduSub BlueROV2 Heavy configuration. The main ballast is a removable steel plate at the lowest point, providing a low centre of gravity and improved passive roll stability. The frame is symmetric about all principal axes.

Estimated dry mass is approximately 35 kg; the vehicle is tuned to slightly negative buoyancy (≈100–200 g resultant downward force when submerged) to comply with the competition positive buoyancy requirement when the kill switch is activated. Each thruster generates approximately 1.2 kgf (11.8 N); critical load paths were verified by static pull tests before vehicle integration.

Trade-off: An enclosed hull would reduce drag but significantly increases cost, complexity, and reduces access to internal components. For a first prototype operating at low speeds, the open frame was preferred for its serviceability. The CAD was developed in Onshape before being standardised in Siemens NX.

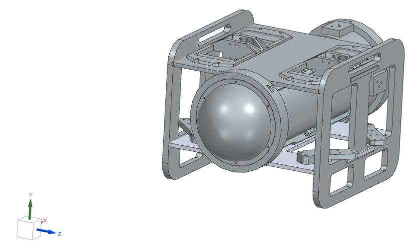

Figure 1: Front view of the AUV showing the spherical acrylic dome and side-plate open-frame structure.

2.2 Materials and Waterproofing

Main structural plates and thruster arms are printed in PLA; components requiring improved water resistance use PETG or ABS with additional sealing. All payload actuator bodies (dropper chambers, torpedo launchers) are printed in ASA for superior UV and moisture resistance. Total mechanical material cost did not exceed approximately 5 000 PLN.

All sealed printed parts are treated with epoxy resin and Dichtol (DIAMANT Polymer GmbH) to close micropores characteristic of FDM printing. The pressure hull uses a three-stage sealing system: a primary O-ring, a roofing-sealant separation layer, and an outer moulding-silicone bead. The acrylic front dome is screwed to the tube flange with six M4 screws torqued with a calibrated torque wrench and additionally potted with epoxy resin. The rear plug is sealed with 166 mm and 190 mm O-rings compressed by hook-fastener clamps. All cable glands and feedthroughs are additionally potted with epoxy. Leak tests confirm submersion at 1 m depth for several hours with no ingress detected.

2.3 CFD Analysis

Fluid-dynamic behaviour of the open frame was analysed in ANSYS 2025R2 (Fig. 2). Streamline visualisation reveals primary drag sources at the pressure hull nose cone and at the horizontal thruster arm junctions. The open frame produces higher drag than an enclosed hull, but the penalty is acceptable at competition operating speeds. Results from the simulation informed minor frame geometry refinements and confirmed structural stiffness margins under peak thruster loads.

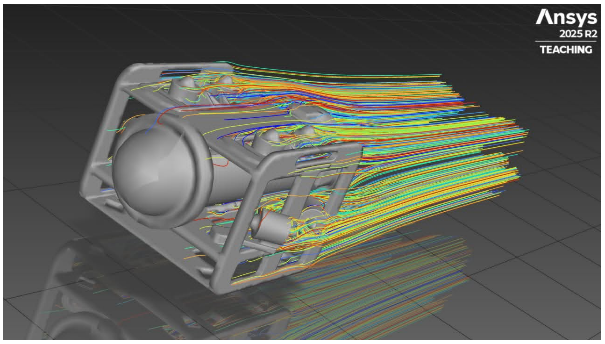

Figure 2: ANSYS 2025R2 streamline visualisation (forward-flow condition). Colour encodes local velocity magnitude; red indicates high-velocity flow around hull nose and thruster arms.

3. Electrical System

3.1 Power Architecture

Two independent battery systems physically isolate propulsion from payload. The main battery—a Tattu 22 000 mAh 4S LiPo (14.8 V nominal, 30C, 1677 g)—is mounted inside the pressure hull and powers propulsion, compute, and navigation. An auxiliary 4S LiPo in a sealed external enclosure powers all RPi nodes, Hailo-8 accelerators, and payload servos. A fault in the external payload chain cannot affect main propulsion or navigation, and vice versa. The main battery is charged via a dedicated connector accessible from outside the hull; a 4S balancer connector and main charge connector are routed through hull penetrations.

Main power flow: battery → two ANL fuse holders (Blue Sea, 300 A each) → Talamex Mini Battery Switch (300 A, IP67) → two Holybro PDB-300A boards in parallel → eight external waterproof ESCs. The parallel PDB arrangement supports up to 200 A peak current (8×25 A) within the 300 A PDB rating. The Pixhawk is powered via a Holybro PM02D module (5.2 V regulated); the Jetson Orin via an external UBEC (6–9.2 V adjustable), providing clean regulated power independent of ESC switching noise. Each RPi 4 + Hailo-8 node has a dedicated UBEC step-down (5 V) from the auxiliary battery; payload servos use an LM2596 step-down (5–6 V) buffered by 2×1000 μF electrolytic capacitors against inrush transients. The complete power distribution is summarised in Table 2.

Table 2: Power Distribution Summary

B.	Rail	Consumer	Path
Main	14.8 V	8× ESC	Batt.→fuse→ kill→PDB
	5.2 V	Pixhawk	Batt. → PM02D
	6–9 V	Jetson Orin	Batt. → UBEC
	5 V	Switch, compass	Baseboard reg.
Aux.	5 V	4× RPi 4+Hailo	Aux.→4×UBEC
	5–6 V	PCA9685+servos	Aux. → LM2596

3.2 Kill Switch and Servo Control

The mechanical Talamex switch (IP67) is mounted externally with clear marking visible to the safety diver. It provides verifiable fail-safe disconnection with no dependency on software state—preferred over an active MOSFET circuit whose gate fault could prevent de-energisation. Upon activation, thruster power is cut within 1 s; the compute stack remains online; thrusters do not spin upon power restoration without explicit command.

All four payload servos (marker dropper ×2, torpedo launcher ×2) are controlled through a single Adafruit PCA9685 Servo Bonnet (I^2C address `0x40`) in a sealed mineral-oil-filled ASA enclosure. A single 6-wire shielded cable (I^2C + power) passes through one hull penetration to the Jetson, replacing four individual long PWM runs.

3.3 Compute and Connectivity

High-level autonomy runs on an NVIDIA Jetson Orin connected to a Holybro Pixhawk + Jetson baseboard (126×80×38 mm). Each camera is paired with a dedicated RPi 4 + Hailo-8 node (26 TOPS) housed in a sealed external enclosure. An internal TP-Link LS1005G Gigabit switch interconnects all Ethernet nodes. A DroneCAN RM3100 compass provides heading reference. All hull penetrations use Weipu WK20 IP68 connectors; cable pass-throughs use Blue Robotics

WetLink JPT penetrators. *Trade-off—distributed vs. centralised vision:* dedicated RPi + Hailo nodes bound per-camera inference latency independently of Jetson load and provide fault isolation, at the accepted cost of increased network complexity.

4. Sensors & Payload Actuators

4.1 Vision System

Two cameras provide environmental awareness: a forward-facing camera for gate classification, obstacle detection, and torpedo targeting; and a downward-facing camera for path-marker following and bin localisation. Each camera is paired with a dedicated RPi 4 + Hailo-8 node running inference locally at >15 fps. Only structured detection results are forwarded over Ethernet to the Jetson. Failure of one camera node does not impair the other.

4.1.1 Synthetic Training via Gaussian Splatting

A key challenge in underwater object detection is the scarcity of annotated training data and the domain gap caused by water turbidity, absorption, and scattering. We developed a synthetic data pipeline based on 3D Gaussian Splatting (GS).

Scene capture: Multi-view image sequences were recorded in a pool environment with sufficient inter-frame overlap for reliable Structure-from-Motion reconstruction.

Reconstruction: Sequences were processed through COLMAP for camera pose estimation, then through OpenSplat to produce 3D Gaussian Splat scene representations.

Novel view synthesis: New camera trajectories were sampled and rendered from the splat representations, producing photorealistic images from viewpoints not present in the original capture.

Turbidity augmentation: Wavelength-dependent absorption and scattering were applied at three intensity levels per rendered image, simulating varying water clarity conditions.

Training and results: Annotated synthetic images were combined with real data to augment the YOLOv8 training set. Four conditions were compared: baseline real-data only; GS-augmented same-medium; GS-augmented varied turbidity; and GS-only. Training ran on PLGrid Athena (NVIDIA A100 GPUs). The varied-turbidity condition achieved the highest mAP@0.5 on real-image test data, confirming that turbidity diversity in synthetic training improves generalisation to unseen pool conditions.

4.2 Depth and Altitude Sensors

A Blue Robotics Bar30 high-resolution pressure sensor (I^2C, 300 m rated) provides absolute depth measurement fused with Pixhawk IMU data in the MAVROS localisation pipeline. A downward-facing Blue Robotics Ping Sonar (single-beam, 100 m range, 25° beam, UART) provides altitude above the pool floor during the Bins task, preventing bottom strikes during approach and positioning. Acoustic ranging was selected over optical alternatives because it is unaffected by water turbidity and pool lighting. Reserved mounting positions exist for a forward-facing Ping Sonar (obstacle avoidance) and a DVL (velocity estimation) in future iterations.

4.3 Hydrophone Array

Task V requires navigating to an acoustic pinger at 25–40 kHz. Three Aquarian AS-1 hydrophones (1 Hz–100 kHz, 200 m rated) are mounted in an equilateral triangle on the underside of the frame with a minimum 15 cm baseline. Each connects to a dedicated analogue front-end: an INA128P instrumentation amplifier followed by a TL072 active bandpass filter tuned to 25–40 kHz. A Teensy 4.1 simultaneously samples all three channels (≈500 kSps per channel, 12-bit ADC), computes Time Difference of Arrival (TDOA), and outputs a bearing to the Jetson via UART. *Trade-off:* Bearing-only localisation from three hydrophones is sufficient for pinger approach; four-element TDOA for range estimation is scoped for a future iteration.

4.4 Marker Dropper and Torpedo Launcher

Task III requires releasing two golf-ball markers (42.67 mm, ≈45 g) into target bins. A dual-chamber gravity-release dropper is mounted on the underside payload plate. Each chamber is sealed by a servo-actuated ASA-printed gate disc

(PowerHD LW-13MG, waterproof, 35 kg·cm at 6 V) rotating 90° to release the ball. Chambers are positioned 40 mm apart for independent targeting of adjacent bin halves. Payload actuators are summarised in Table 3.

Table 3: Payload Actuator Summary

Actuator	Model	Ch.	Function
Dropper L	LW-13MG	0	Release left marker
Dropper R	LW-13MG	1	Release right marker
Torpedo L	LW-13MG	2	Release left torpedo
Torpedo R	LW-13MG	3	Release right torpedo

Task IV requires firing two torpedoes through openings in a vertical target board from up to 1.5 m. A dual-tube spring-loaded launcher is mounted forward of the dropper. Each 30 mm ASA-printed tube is lined with a PTFE sleeve to reduce friction. A servo-actuated latch retains a compressed steel spring; 45° servo rotation launches the torpedo. Torpedoes are printed in ASA, ballasted with lead shot for neutral buoyancy, and designed with the centre of pressure rearward of the centre of gravity for passive trajectory stabilisation. Aiming is achieved by vehicle yaw. *Trade-off vs. pneumatic:* the spring launcher requires no on-board gas supply, pressure vessel, or depth compensation, at the cost of fixed launch velocity. For 1.0–1.5 m distances, spring energy is sufficient.

5. Software Architecture

5.1 Overview and Functional Domains

The software architecture is a modular, distributed framework built on ROS 2 Humble, running in a containerised environment on the Jetson Orin. Communication between modules uses custom `bluespark_interfaces` messages for low-latency data exchange. Four functional domains are defined.

The **Perception Domain** provides environmental awareness via the `vision_node` for object detection and the `depth_estimator_node` for vertical localisation, publishing high-level spatial coordinates to the navigation stack.

The **Navigation and Control Domain** orchestrates physical movement. The `movement_node` processes real-time perception data, determines the current objective based on mission state, and issues movement commands to lower-level orientation nodes. The `depth_hold_node` implements a PID-based control loop for depth maintenance. These signals converge at the `rc_override_node`, which multiplexes autonomous setpoints and manual safety overrides for the MAVLink-compatible flight controller. The simplified system architecture is shown in Fig. 3.

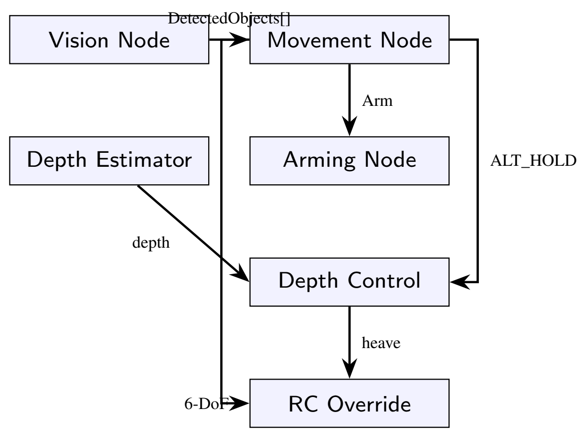

Figure 3: Simplified ROS 2 node architecture.

5.2 Perception Pipeline

The `vision_node` publishes a `DetectedObjectArray` message per frame. Each `DetectedObject` entry includes: classification label and confidence score; 3D coordinates (x, y, z) relative to the camera frame, computed via a pinhole camera model with real-world object dimensions defined in `object_config.json`; horizontal and vertical angles relative to the optical centre (used notably for gate traversal heading alignment); and bounding box centre coordinates for tracking and debugging.

The AUV implements a dynamic priority system for perception. While the frontal camera serves as the main sensor for long-range navigation, the system transitions to the downward camera during close-proximity tasks such as precise positioning over floor markers. Depending on the current mission state, the AUV filters detections—gate detection is prioritised during the Gate Traversal phase, suppressing peripheral noise. LIDAR supplements vision for floor-distance measurement during tasks requiring precise low-altitude operation.

5.3 Mission Planner

End-to-end mission sequencing from initial arming to final surfacing is orchestrated by a Behavior Tree (BT) architecture built on the `py_trees` framework. BTs were preferred over Finite State Machines (FSMs) for modularity: FSMs become tightly coupled and difficult to modify without rewriting multiple state transitions, while BTs allow rapid addition, removal, or reordering of mission nodes without cascading changes.
Trade-off—Python vs. C++: Python was chosen over C++ for faster iteration at mission-management frequencies.

6. Testing & Validation

6.1 Pre-dive Checklist

The following mandatory checks are performed before every pool test:

1. **Seal test:** Full submersion in a 1000-litre tank for $\geq$10 min. After retrieval, the pressure hull end caps and all cable penetrations are inspected for moisture. Any ingress triggers resealing before proceeding.
2. **Kill switch:** Physical activation confirmed to cut thruster power within 1 s; compute confirmed to remain online; re-arm confirmed not to spin thrusters until explicitly commanded.
3. **Bench actuation:** Each servo cycled once in air (dropper gate, torpedo latch); correct motion and return confirmed.
4. **Vision check:** Both RPi + Hailo nodes confirmed publishing detection topics at $>$15 fps; test image produces non-empty bounding box output.
5. **Hydrophone check:** Teensy confirmed publishing bearing topic; reference tone at known azimuth verified within $\pm 15^\circ$.
6. **Thruster check:** All eight thrusters commanded to low duty cycle in air; all confirmed spinning in correct direction.

6.2 Subsystem Validation

Marker dropper: Ten drop trials per chamber over a 200 mm aperture target. Success criterion: $>$90% balls pass through the aperture. Gate disc geometry is iterated until criterion is met.

Torpedo launcher: Ten shots per tube toward a 150 mm aperture at 1.0 m distance. Success criterion: $>$80% shots pass through aperture; vertical drift $<$50 mm over 1.0 m flight. Ballast mass is iterated until neutral buoyancy and trajectory stability are achieved.

Hydrophone system: Reference pinger placed at known azimuths (0°, 90°, 180°, 270°) at 2 m distance. Success criterion: mean bearing error $<15^\circ$ at all azimuths. Results are used to calibrate the TDOA geometry model.

Vision system: Detection models evaluated on held-out real pool images across four training conditions: baseline real-data only, GS same-medium, GS varied-turbidity, and GS-only. Primary metric: mAP@0.5 on real-image test set. Secondary metric: detection rate vs. simulated range with turbidity augmentation at increasing intensities.

Full mission integration: End-to-end pool runs executing each primary task in sequence with the mission planner running autonomously. Success criterion: vehicle completes Gate traversal, path-marker following, and bin drop without human intervention within 15 min.

6.3 Safety Compliance

Prior to competition submission the following are verified and documented: kill switch de-energises thrusters within 1 s; vehicle exhibits positive buoyancy ($>$0.5% of dry mass) when kill switch is activated; all thruster guards installed with $\geq$51 mm clearance; battery voltage $\leq$60 VDC open circuit; no materials released into pool water except markers and torpedoes.